Supporting Information

Surface Specifically Modified NK-92 Cells with CD56 Antibody Conjugated Superparamagnetic Fe_3O_4 Nanoparticles for Magnetic Targeting Immunotherapy of Solid Tumor

Songbo Zhao[a,1], Jiazhi Duan[b,1], Yalin Lou[a], Ruyun Gao[a], Shanshan Yang[a], Piming Wang[c], Chunhua Wang[d], Lin Han[d], Minghuan Li[e], Chunhong Ma[a], Xiaohong Liang[a], Hong Liu[b,*], Yuanhua Sang[b,*], Lifen Gao[a,*]

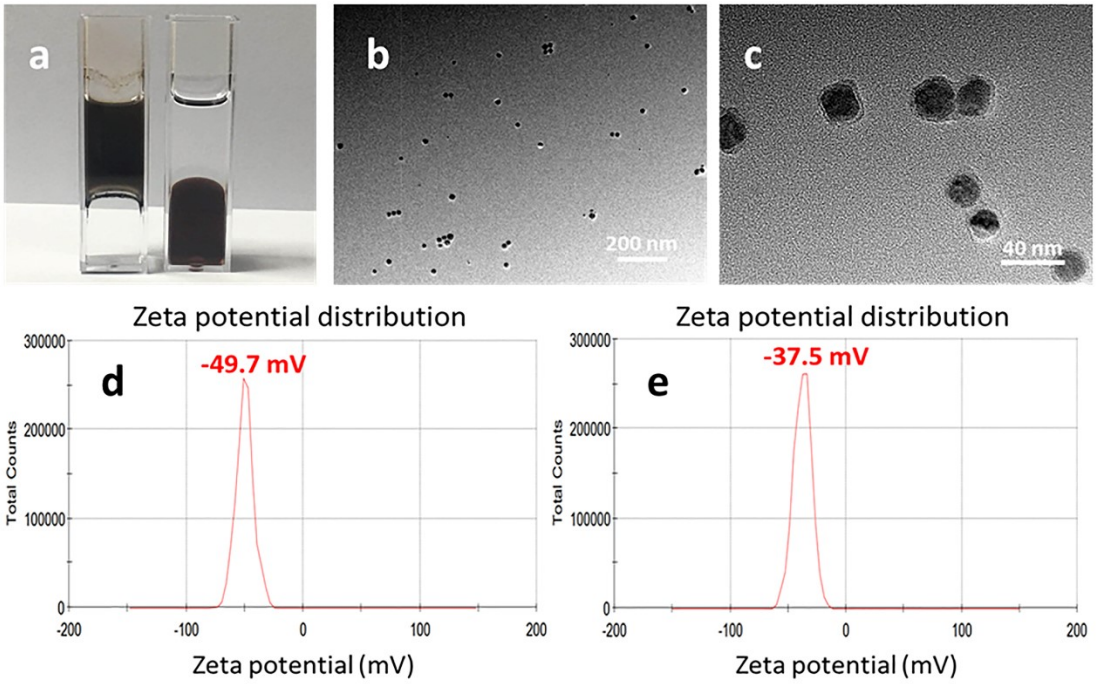

Figure S1. Characterization of synthesized Fe_3O_4-DMSA and Fe_3O_4-CD56 nanoparticles (a) The phase inversion of Fe_3O_4 from hexane (top) to water (bottom) after the modification of DMSA molecular. **(b)** The TEM image of synthesized Fe_3O_4-DMSA nanoparticles. **(c)** The TEM image of Fe_3O_4-CD56 nanoparticles at high magnification. **(d)** and **(e)** The Zeta potential distribution of Fe_3O_4-DMSA and Fe_3O_4-CD56 nanoparticles.

The Fe_3O_4 synthesized in octadecene could be dispersed well in hexane but not be

dispersed in water, after the modification of DMSA molecular on the surface of Fe_3O_4 nanoparticles, the Fe_3O_4-DMSA nanoparticles become water dispersive (Figure S1a). Due to the abundant carboxyl group of DMSA molecular, the Fe_3O_4-DMSA nanoparticles show an excellent monodispersity in water, which could be observed in Figure S1b. Moreover, the carboxyl group enable the coupling with CD56 antibody. After the coupling of CD56 antibody, there exists a surface coating on the surface of Fe_3O_4-DMSA nanoparticles (Figure S1c). The carboxyl groups on the surface of Fe_3O_4 determine the large zeta potential value, which enable the excellent water dispersibility and long-term preservation. The coupling of CD56 antibody consumes the carboxyl group, which decrease the zeta potential value to -37.5 mV.

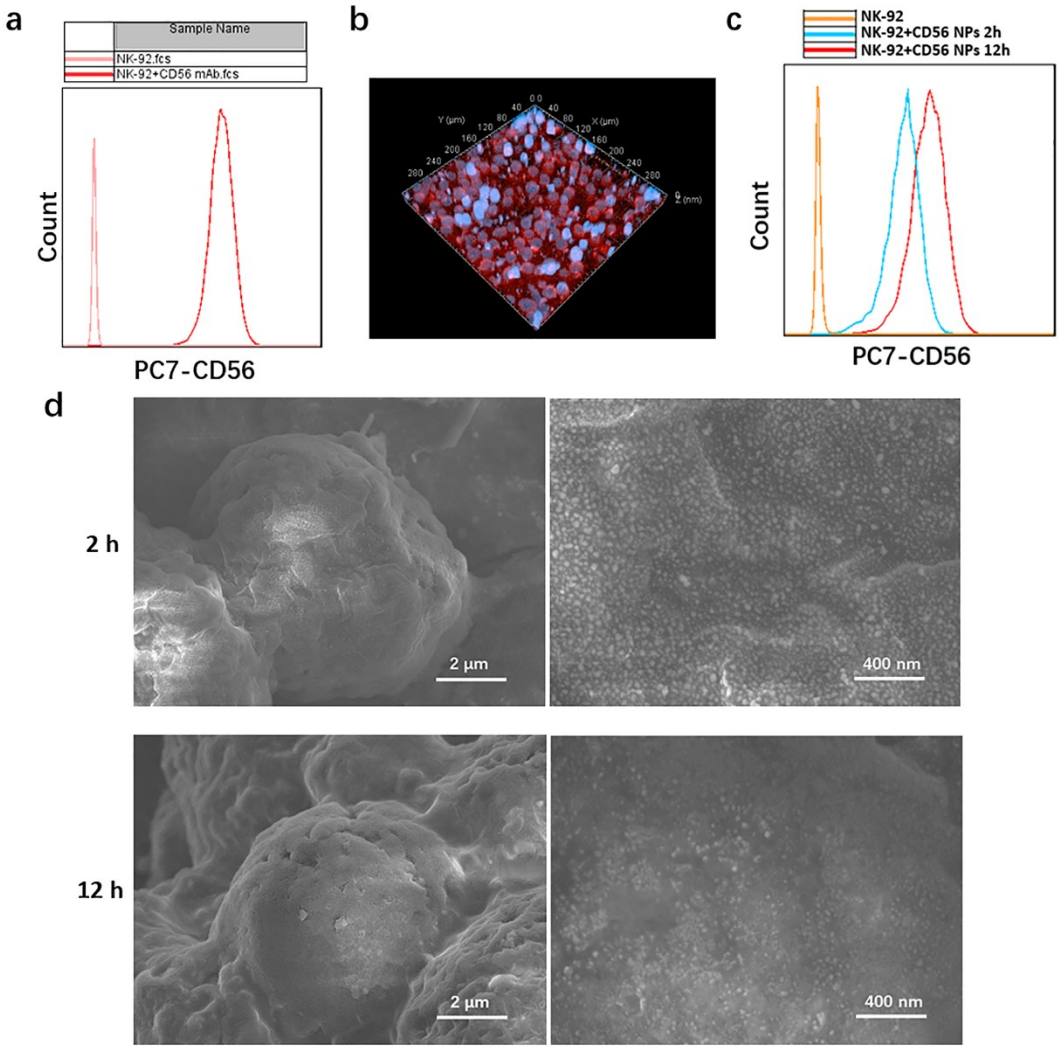

Figure S2. The Pe/Cy7-conjugated CD56 NPs could be bound to the surface of NK-92 cells for a long time (a) NK-92 cells were highly express CD56 antigen. **(b)** The three-dimensional diagram of NK-92 cells combined CD56 NPs detected by confocal microscopy. NK-92 cells were co-cultured with CD56 NPs and they were still bound at 2 hours and 12 hours, which were presented by flow cytometry **(c)** and SEM **(d)**. SEM: scanning electron microscope.

We also confirmed that the NK-92 cells highly expressed CD56 molecular analyzed on a flow cytometer (Figure S2a). The 3D confocal laser scanning image of Fe_3O_4-CD56 and NK-92 cells complex further confirmed the specific targeting effect of Fe_3O_4-CD56 NPs toward NK-92 cells in three dimensional spaces, and the red fluorescence light of CD56 NPs around the NK cell nucleus showed that the CD56 NPs could be specifically

bound to the NK-92 cell surface (Figure S2b). To confirm the binding strength and time between the NK-92 cells and CD56 NPs, the flow cytometry and SEM were used to characterize the binding state after the incubation of CD56 NPs and NK-92 cells for 2 hours and 12 hours. The flow cytometry result (Figure S2c) showed that the fluorescent labeling still existed on the surface of NK-92 cells after 2 hours and even 12 hours. The SEM images of CD56 NPs and NK-92 cells complex after 2 hours incubation showed that there existed large amount of Fe_3O_4 nanoparticles on the surface of the NK-92 cells. After 12 hours incubation, there still existed large but fewer amount of Fe_3O_4 nanoparticles on the cell surface (Figure S2d), which indicated that the binding between NK-92 cells and CD56 NPs was very lasting.

In addition, the number of nanoparticles combined with NK-92 cells could be calculated according to following method. The known parameters of Fe_3O_4 nanoparticles: r=10 nm, ρ=5.18 g/cm³. The known parameters of CD56 antibody: 0.2 mg/mL, 150 kDa. MFI=2.1×10^5. According to the synthesis method, 4 mg Fe3O4 nanoparticles were reacted with 100 μL CD56 antibody.

The Fe_3O_4 particles number: $4\times10^{-3}\div[4/3\times\pi\times(10\times10^{-9})^3\times5.18\times10^{-6}]\approx1.84\times10^{14}$

The CD56 antibody number: $6.02\times10^{23}\times(2\times10^{-7}\times100)\div150\approx8.03\times10^{16}$

$n=2.1\times10^5\times1.84\times10^{14}\div(8.03\times10^{16})\approx481$

Therefore, the average number of nanoparticles combined with NK-92 cells was about 481.

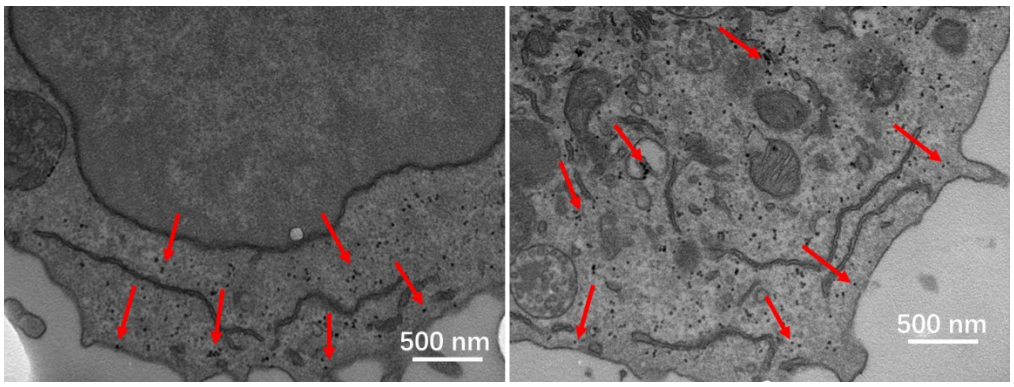

Figure S3. The TEM images after Fe_3O_4-CD56 nanoparticles combining NK-92 cells for 2 h (left) and 12 h (right).

The TEM (transmission electron microscopy) images after Fe_3O_4-CD56 nanoparticles combining NK-92 cells for 2 h and 12 h was performed to confirm the specifically targeting effect and cell uptake behavior. As shown in the image, the nanoparticles appeared in the cell, which efficiently indicated that the Fe_3O_4-CD56 nanoparticles could specifically combine with NK-92 cells and be taken by NK-92 cells after specific combination for 2 h and 12 h.

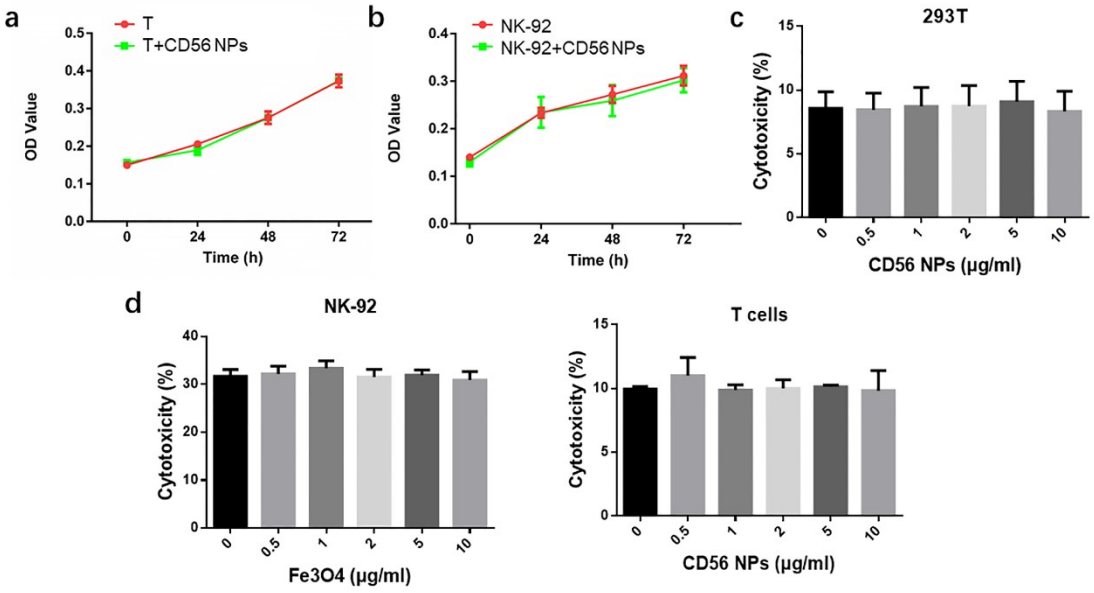

Figure S4. (a) NK-92 cells highly expressed CD56 antigen **(a)** the proliferation ability of human T cells was not affected by CD56 NPs. **(b)** The proliferation analysis of NK-

92 cells combined CD56 NPs using CCk-8 method. **(c)** The toxicity of CD56 NPs towards HEK293T cells and human T cells. **(d)** The cytotoxicity of NK-92 cells conjugated with Fe_3O_4 NPs towards K562 cells.

The CD56 NPs and CD56-negative T cells were co-cultured and CCK-8 experiment was established (Figure S4a). Meanwhile, The CD56 NPs and NK-92 cells were co-cultured and CCK-8 experiment was established (Figure S4b). The results showed no difference of growth curve between T cells or NK-92 cells combined with or without CD56 NPs. These data indicated that the proliferation ability was not affected when the CD56 antibody bound to T cells or NK-92 cells. In addition, CD56 NPs had no toxicity to human T cells and HEK293T cells (Figure S4c) and The Fe_3O_4 NPs had no effect on the killing ability of NK-92 to K562 cells (Figure S4d).

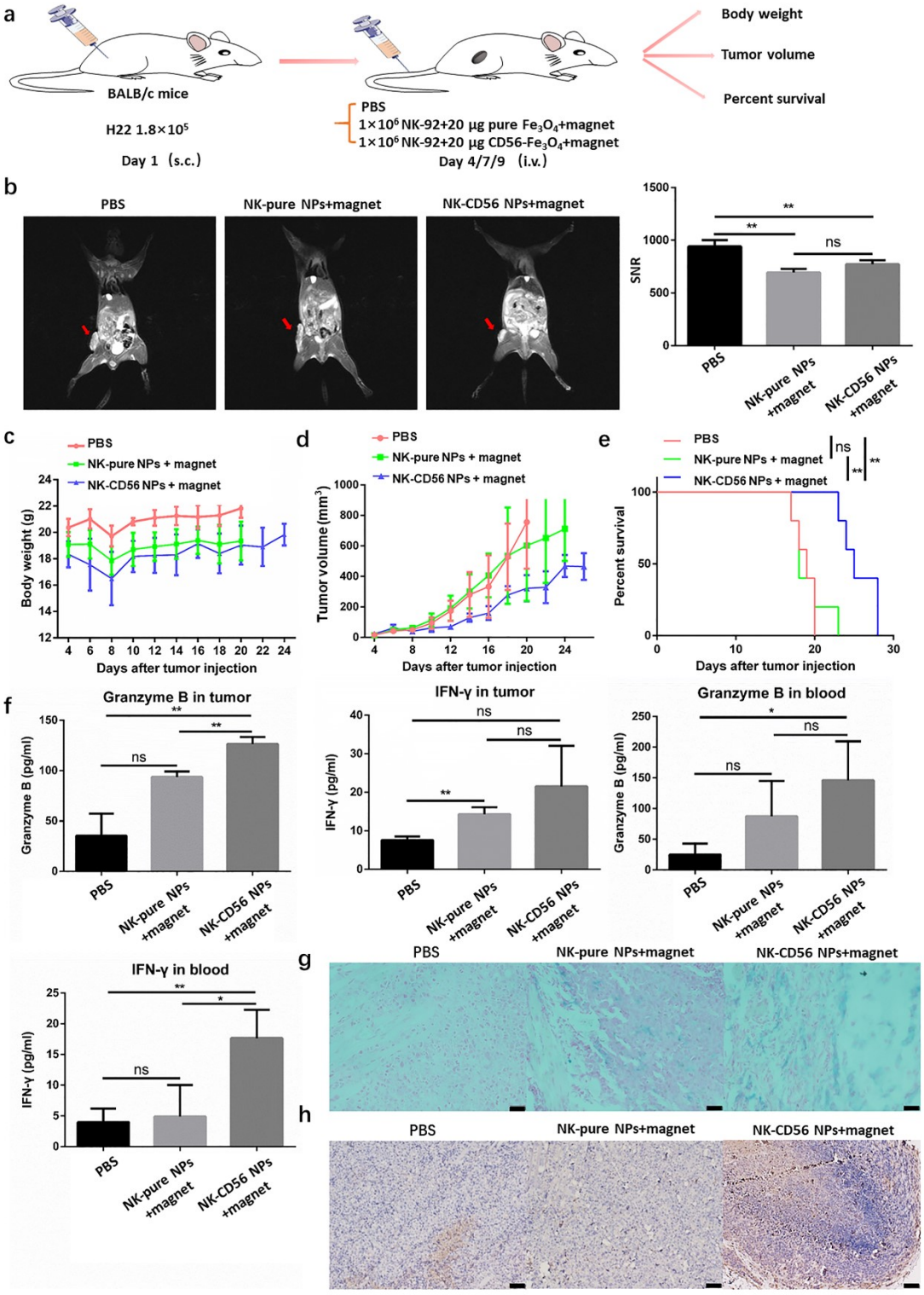

Figure S5. The antitumor activity of NK-CD56 NPs biohybrid plus magnet in BALB/c H22 mouse model. (a) Experimental design. **(b)** The picture of tumors and SNR accounting for quantity of Fe_3O_4 NPs infiltrated by T_2 channel were presented on day 10 using MRI. (SNR: Signal to Noise Ratio. MRI: magnetic resonance imaging.) **(c)** Body weight change of tumor-bearing mice after NK-92 cells transfer. Weight per mouse was normalized to starting weight pre-NK-92 cells transfer. **(d)** Tumor volume

of the mice was measured once every two days. **(e)** Mice were humanely sacrificed when tumors reached 12 mm in diameter. Survival was evaluated from the first day of tumor injection until death. **(f)** Enhanced release of Granzyme B and IFN-γ as NK-CD56 NPs biohybrid in response to tumors. **(g)** Prussian blue staining of tumor tissues extracted from treated with PBS, NK-pure NPs and NK-CD56 NPs biohybrid on day 16. Magnification: ×400. (Scale bar 50 μm). **(h)** Immunohistochemistry slides of subcutaneous xenograft sections from all groups were presented. The human CD45 antigen were detected in NK-CD56 NPs group. Magnification: ×400. (Scale bar 50 μm). All the values are presented as the mean±standard error of the mean，and statistical analysis was performed using the log-rank (Mantel-Cox) text. *p＜0.0, **p＜0.01, compared with controls.

The female BALB/c nude mice were subcutaneously injected with H22 cells. The control groups received tail injection of PBS or NK-pure NPs complex, while the experimental groups received injection of NK-CD56 NPs complex (Figure S5a). The T_2 MRI signals reveal the existence of Fe_3O_4 NPs in tumors in the NK-pure and NK-CD56 NPs groups compared with the PBS group (Figure S5b). The body weights of NK-CD56 NPs group were slightly less than the other groups, and it might be due to the existing of tumors (Figure S5c). The tumor growth of NK-CD56 NPs group are distinctly suppressed compared to that of control groups. Moreover, the result was also reflected in the survival of the mice (Figure S5d and S5e), with the reason that the presence of infiltrating NK-92 cells in experiment group (Figure S5h). The prussian blue staining shows more Fe_3O_4 in the tumors of NK-pure and NK-CD56 NPs groups (Figure S5g). The NK-92 cells from NK-CD56 NPs groups released more Granzyme B and IFN-γ in tumor and serum compared to control groups (Figure S5f).

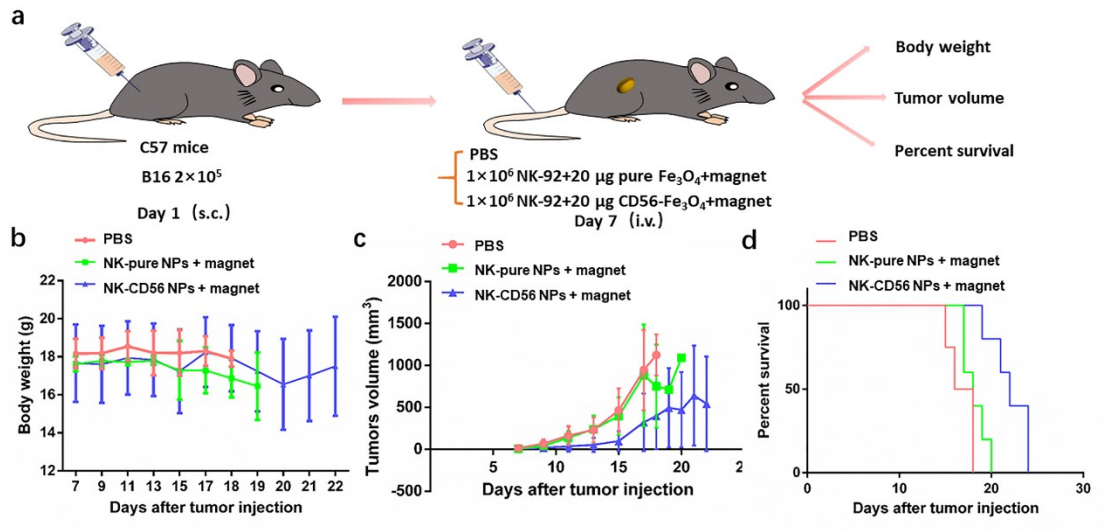

Figure S6. The antitumor activity of NK-CD56 NPs biohybrid plus magnet in B16 mouse model. (a) Experimental design. **(b)** Body weight change of tumor-bearing mice after NK-92 cells transfer. Weight per mouse was normalized to starting weight pre-NK-92 cells transfer. **(c)** Tumor volume of the mice was measured once every two days. **(d)** Mice were humanely sacrificed when tumors reached 15 mm in diameter. Survival was evaluated from the first day of tumor injection until death.

The female C57BL/6N mice were subcutaneously injected with B16 cells. The control groups received tail injection of PBS or NK-pure NPs complex, while the experimental groups received injection of NK-CD56 NPs biohybrid (Figure S6a). The body weights of NK-CD56 NPs group were slightly less than the other groups, and it might be due to the existing of tumors (Figure S6b). The tumor growth of NK-CD56 NPs group were distinctly suppressed compared to that of control groups. Moreover, the result was also reflected in the survival of the mice (Figure S6c and S6d).